TreeDimensional Journal, Vol. 16, e025287, 2026
Original Article | DOI: https://doi.org/10.55746/treed.2026.01.287

Automated estimation of tree number in *Pinus elliottii* Engelm. and *Eucalyptus* sp. plantations using UAV imagery

Paula Campos Bonatto[1,*], Adriano Luis Schunemann[1], Gabriel Paes Marangon[1], Gerson dos Santos Lisboa[2], Pietro Pimentel Morales Duran[1]

Abstract
Forestry activities require accurate inventories to support sustainable forest management; however, conventional field-based inventories are costly and difficult to implement over large areas. This study aimed to define and evaluate a methodology to estimate the number of trees in commercial plantations of *Pinus elliottii* and *Eucalyptus* sp. using images acquired by an Unmanned Aerial Vehicle (UAV) in the central region of Rio Grande do Sul, Brazil. The study was conducted in three plantations (P1 – *Pinus*, 17 ha; P2 and P3 – *Eucalyptus*, totaling 33 ha). Circular sampling plots of 400 m² were established for the conventional forest inventory. Orthomosaics were generated from UAV flights using a DJI Mavic 3M at 120 m altitude, with 80% forward and 70% side overlap. Circular and rectangular sampling units with the same area were delineated on the images at the same sampling locations. Image processing was performed in Agisoft Metashape, and spatial analysis was conducted in QGIS. Tree counts obtained by the three methods (field inventory, circular plots on imagery, and rectangular plots on imagery) were compared using the Shapiro–Wilk normality test and, when appropriate, Student's *t*-test or the Mann–Whitney *U* test. Statistically significant differences were observed between field-based counts and UAV-derived estimates in all study areas, whereas no significant differences were found between the two image-based methods. Discrepancies were smaller in *Pinus* plantations and more pronounced in *Eucalyptus* stands, indicating underestimation related to crown architecture, stand density, crown overlap, and image resolution and illumination constraints. Under the evaluated conditions, UAV-based approaches were not efficient for sample-based estimation of tree numbers, highlighting the need for species-specific calibration, lower-altitude flights, and improved image processing strategies.

Keywords
Forest Inventory — Drone — *Pinus* — *Eucalyptus* — Remote Sensing

[1] *Federal University of Pampa*
[2] *Federal University of Goiás*
***Corresponding author**: paulacampos.aluno@unipampa.edu.br

1. Introduction

Forestry activities play an essential role in the development of society, influencing quality of life, promoting economic development, and, when conducted in accordance with the principles of sustainable management, contributing significantly to the conservation of natural resources by enabling the balanced and responsible use of forests. Therefore, for the planning and execution of any technical operation aimed at the rational use of forest resources, it is necessary to know and accurately quantify these resources.

Forest inventory is the main tool used for this purpose, serving as the basis for acquiring quantitative and qualitative information within a given area. Although traditional forest inventory provides highly accurate estimates of a population, it also presents operational difficulties and high costs (Pinto et al., 2024).

Thus, new technologies have been increasingly employed in forest area surveys with the aim of reducing costs, facilitating data collection, and increasing the reliability of the information obtained. Several authors, such as Figueiredo et al. (2018), Sousa (2017), and Corte et al. (2020), highlight the use of remote sensing and machine learning algorithms in the acquisition and processing of forest data.

Remote sensing technology is applied through Unmanned Aerial Vehicles (UAVs), popularly known as drones, which offer a wide range of applications. These UAVs are widely used in agriculture and have gained prominence in forest management with the goal of optimizing operational routines and reducing costs (Figueiredo et al., 2018). According to the same authors, precision management, or Forestry 4.0, has been applied, for ex-

Received: 2025/11/12 | **Accepted:** 2026/01/30 | **Online published:** 2026/01/31

ample, in semi-automated forest inventories.

According to Han et al. (2022), aerial image mosaicking techniques have been widely used in recent decades for activities such as monitoring, forest fire detection, tree counting, among others. Information on the location, shape, and condition of trees is fundamental for precision management. Advances in UAV-based technologies have supported improvements in methods for identifying and quantifying trees.

However, further studies and methodologies are still required to demonstrate the efficiency of these tools. Therefore, the objective of this study was to define a methodology for estimating the number of trees in commercial plantations of *Pinus* and *Eucalyptus* species using UAVs in the central region of Rio Grande do Sul, Brazil.

2. Materials and Methods

2.1 Characterization of the study areas

The study was carried out in three forest plantations located in two different areas. The first, referred to as plantation 1 (P1), is located in Santa Margarida do Sul, Rio Grande do Sul, Brazil (Figure 1 – b and c), and covers an area of 17 ha planted with *Pinus elliottii*, at latitude $30°20'20.5''$ S and longitude $54°00'21.3''$ W. The stand was established in 2008, with a spacing of 2.5 m between trees and 4.0 m between rows.

According to Moreno (1961), based on the Köppen climate classification, the climate in Santa Margarida do Sul is subtropical, classified as type Cfa. Winds have an average speed of around 10 km h^{-1} and, in the Campanha region, predominantly follow a southwest direction throughout most of the year. The region is characterized by a mean annual precipitation ranging between 1,300 and 1,600 mm.

According to Raffaelli (2002), the soils of the municipality are classified into two main types. One corresponds to Planosols with medium texture, occurring on flat to gently undulating relief over recent sedimentary substrates. The other type consists of Litholic soils with medium texture, which occur on undulating relief and are associated with a granitic substrate.

The second and third stands, referred to as plantation 2 (P2) with 8 ha and plantation 3 (P3) with 25 ha, respectively, consist of *Eucalyptus* sp. and are located in the municipality of Lavras do Sul, Rio Grande do Sul (Figure 1 – b and d).

The study was conducted in the municipality of Lavras do Sul, Rio Grande do Sul, located in the Southern Rio Grande do Sul Shield, where soils are classified as Litholic Neosols, suitable for livestock production and reforestation (MSRS, 2024). According to the Köppen climate classification, the region has a humid subtropical climate (Cfa), with mean annual temperatures ranging from $16°C$ to $18°C$ (Macedo, 1984).

The vegetation in Lavras do Sul is characterized by a continuous herbaceous cover dominated by grasses. There are no gallery forests; instead, shrubs and trees occur in a scattered manner or grouped in small patches (*capões*), and the vegetation is classified as Grassy–Woody Savanna (IBGE, 2012).

The studied area comprises 33 hectares of *Eucalyptus* plantations without thinning, divided into two sections: area 1 (P2), with 8 hectares, established in 2012, with a spacing of 2.0 × 2.0 meters and using a mix of genetic material; and area 2 (P3), with 25 hectares, established in 2009, with a spacing of 4.0 × 1.5 meters and composed exclusively of the species *Eucalyptus dunnii* Maiden.

To carry out this study, aerial surveys were conducted using an unmanned aerial vehicle (UAV) (DJI brand, DJI Mavic 3M model), presented in Table 1, along with conventional forest inventories in the three plantations.

Table 1. Characteristics of the DJI Mavic 3M UAV used in the P1, P2, and P3 areas of *Pinus* and *Eucalyptus* plantations in the municipalities of Santa Margarida do Sul and Lavras do Sul, Rio Grande do Sul, Brazil.

Parameter	Specifications
Net weight (with propellers and RTK module)	951 g
Maximum takeoff weight	1,050 g
Diagonal length	Diagonal: 380.1 mm
Maximum speed (near sea level, no wind)	15 m/s (normal mode) Forward flight: 21 m/s; lateral flight: 20 m/s; backward flight: 19 m/s (sport mode)
Maximum flight time (no wind)	43 minutes
GNSS	GPS + Galileo + BeiDou + GLONASS (GLONASS is supported only when the RTK module is enabled)
Operating temperature	$-10°C$ to $40°C$
RGB image sensor	4/3 CMOS, effective pixels: 20 MP
RGB lens	Field of view (FOV): $84°$ 35 mm equivalent focal length: 24 mm Aperture: f/2.8 to f/11 Focus: 1 m to ∞
Maximum RGB image dimensions	5280 × 3956
RGB image format	JPEG/DNG (RAW)
Multispectral image sensor	1/2.8-inch CMOS, effective pixels: 5 MP
Multispectral camera bands	Green (G): 560 ± 16 nm Red (R): 650 ± 16 nm Red Edge (RE): 730 ± 16 nm Near Infrared (NIR): 860 ± 26 nm
Multispectral image format	TIFF

Source: Adapted from DJI Mavic 3M (2025).

In P1 (Figure 1a and b), an aerial survey was conducted using a UAV (DJI, model *DJI Mavic 3M*), along with a conventional forest inventory. The Google Earth software was used for the planning and spatial distribution of the sampling plots (Kusnandar, 2020).

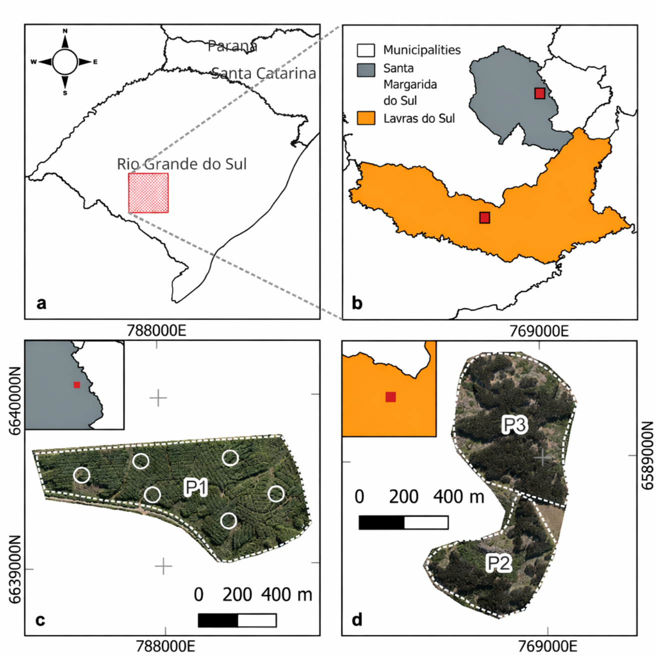

Figure 1. Location of the study areas in plantations P1, P2, and P3 of *Pinus* and *Eucalyptus* in the municipalities of Santa Margarida do Sul and Lavras do Sul, Rio Grande do Sul, Brazil.

Legend: (a) location of the two study areas in Rio Grande do Sul; (b) location of the plantation areas in Santa Margarida do Sul and Lavras do Sul; (c) orthomosaic obtained by UAV at the Pinus sp. plantation site; (d) orthomosaic obtained by UAV at the Eucalyptus sp. plantation site. UTM Coordinate System, SIRGAS 2000 Datum, Zone 21S.

In the forest inventory of P1, 25 circular sampling units were systematically allocated, with an average spacing of 101 m along the planting rows and 84 m between rows. The radius adopted for each sampling unit was 11.28 m, resulting in an area of approximately 400 m² per unit. The sampling units were installed using a digital laser distance meter and subsequently georeferenced with a navigation GNSS receiver (Garmin GPSMAP 76CSx), applying the absolute positioning method (Monico, 2008). This method is used to determine the exact geographic position of a receiver on the Earth's surface (Hofmann-Wellenhof et al., 2001).

In P2, 10 sampling units were allocated, and in P3, 20 sampling units, in order to adequately cover and represent the entire plantation. In the forest inventory, fixed-area circular sampling units of 400 m² were randomly distributed, and their locations were automatically generated using the "random points" procedure within polygons in the QGIS software. After the points were imported into the navigation GPS, they were materialized in the field, where dendrometric data of the trees were collected. Thus, the sampling design was carried out considering individual trees as the variable of interest. A maximum sampling error of 10% was adopted, with a confidence level of 95%.

The variables collected in the field included the diameter at breast height (DBH), measured at 1.30 m above ground level using a mechanical forest caliper, encompassing all trees within the sampling units; and the total height of the first ten trees measured in each sampling unit, determined with the aid of a Vertex IV hypsometer.

The flights were conducted at an altitude of 120 m, with the camera manually configured (camera model FC2204 – 4.386 mm, focal length of 4.386 mm, pixel size of 1.58 × 1.58 µm, ISO 1600, and shutter speed of 1/250), and using automatic flight planning over an area of 17 ha. The flight speed was set to 15 m s^{-1}, with 80% frontal overlap and 70% lateral overlap, resulting in an estimated acquisition of 56 images.

The DJI Mavic 3M UAV is equipped with one RGB camera and four multispectral cameras. The RGB camera captures three bands of the visible spectrum (red, green, and blue) using a 4/3″ CMOS sensor with 20 megapixels. The multispectral cameras are composed of four single-band 1/2.8″ CMOS sensors (5 megapixels), capable of acquiring images separately in the red (650 $\pm$ 16 nm), red edge (730 $\pm$ 16 nm), green (560 $\pm$ 16 nm), and near-infrared (NIR; 860 $\pm$ 26 nm) bands. In addition, the onboard system includes a sunlight spectral sensor positioned on the top of the drone, responsible for monitoring solar irradiance and enabling radiometric correction of reflectance (DJI, 2023).

Flight planning was carried out using the flight planning software integrated into the UAV controller, referred to as "Flight Route," set at an altitude of 120 meters. The flight over the *Pinus* sp. area was conducted on July 24, 2024, between 11:00 a.m. and 1:00 p.m. For the *Eucalyptus* sp. area, the flight took place on July 19, 2024, at the same altitude and within the same time window, using 80% frontal and 70% lateral overlap for both areas. Camera settings were similar for the two areas, using the M3M camera with a focal length of 12.29 mm, ISO 100, shutter speed of 1/240 s, and aperture of f/5.6.

Subsequently, the images were imported and processed using Agisoft Metashape Professional Edition 1.6.0 (AGISOFT, 2020), trial version, in JPEG format, adopting the Universal Transverse Mercator (UTM) coordinate reference system, Zone 21S, and the SIRGAS 2000 datum, as presented in Table 2.

Table 2. Image processing in the Agisoft Metashape software and the parameters used at each processing stage.

Step	Parameter	Specification
1st Alignment	Accuracy	Medium
	Generic Preselection	Enabled
	Key point limit	40,000
	Tie point limit	4,000
	Adaptive camera model fitting	Enabled
2nd Alignment	Accuracy	High
	Generic Preselection	Enabled
	Key point limit	40,000
	Tie point limit	4,000
	Adaptive camera model fitting	Enabled
	Reset current alignment	Enabled
Dense Cloud Generation	Quality	High
	Depth Filtering	Aggressive
	Calculate Point Colors	Enabled
DSM Generation	Datum / Projection	SIRGAS 2000 / UTM Zone 21S
	Source Data	Dense Cloud
	Interpolation	Default
	Point Classes	All
Orthomosaic Generation	Datum / Projection	SIRGAS 2000 / UTM Zone 21S
	Surface	DEM
	Blending Mode	Default
	Enable hole filling	Enabled
Dense Cloud Classification	From	Any class
	To	Ground + Low Points
	Max angle (deg)	15
	Max distance (m)	0.18
	Cell size (m)	100
DTM Generation	Datum / Projection	SIRGAS 2000 / UTM Zone 21S
	Source Data	Dense Cloud
	Interpolation	Default
	Point Classes	Ground

Source: Author (2025).

The orthomosaic was exported in TIFF format for use in post-processing. The steps performed, along with their respective activities and generated products, are summarized in Figure 2.

For the present study, the number of trees was counted in the plantations (P1, P2, and P3) located in the municipalities of Santa Margarida do Sul and Lavras do Sul, in the state of Rio Grande do Sul, Brazil.

In order to perform tree counts using an alternative method, that is, based on images obtained by the UAV, aerial surveys were conducted over the two study areas.

The maps and the spatial representation of the sample areas where tree counts were performed, as well as the location of the sampling units (Figure 3), were produced using the QGIS software (QGIS Development Team, 2021).

2.2 Sampling

Three methods were defined and compared to estimate the number of trees in the two study areas (Figure 3 – c and d). For the traditional method, a field inventory was conducted in which circular plots were established and the number of trees in each plot was counted. For the

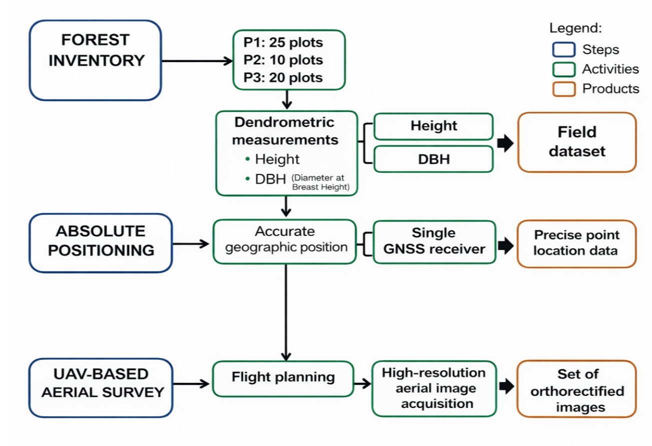

Figure 2. Diagram of the steps, activities, and products generated up to the UAV-based aerial survey in the plantations of areas P1, P2, and P3.
Source: Author (2025).

alternative methods, circular (Figure 3 – a, c, and e) and rectangular (Figure 3 – b, d, and f) plots were delineated on the orthomosaics obtained from UAV imagery. Efforts were made to delineate the plots used in the alternative methods at the same locations where the field inventory was carried out.

For the comparison among methods, the number of trees was counted using rectangular and circular sample plots, each corresponding to an area of 400 m².

The locations where sampling was conducted were defined *a priori*, and their coordinates were determined using a navigation GNSS receiver, which has an approximate positional accuracy of 5 m ($\sigma \simeq 5.00$). For each method, the center of the sampling unit was positioned at the recorded coordinates, and subsequently the geometric shape of the plot was defined in QGIS (Figure 1).

2.3 Statistical analysis

For the statistical analysis, a script was developed using the R statistical computing environment (R Core Team, 2025).

First, the assumption of normality for the tree count values was evaluated using the Shapiro–Wilk test (Shapiro & Wilk, 1965; Royston, 1982a; Royston, 1982b; Royston, 1995). For all groups, when a p-value > 0.05 was obtained, it was possible to state that the sample originated from a population following a normal distribution. In such cases, normality was assumed and the Student's *t*-test (R Core Team, 2025) was applied to compare means.

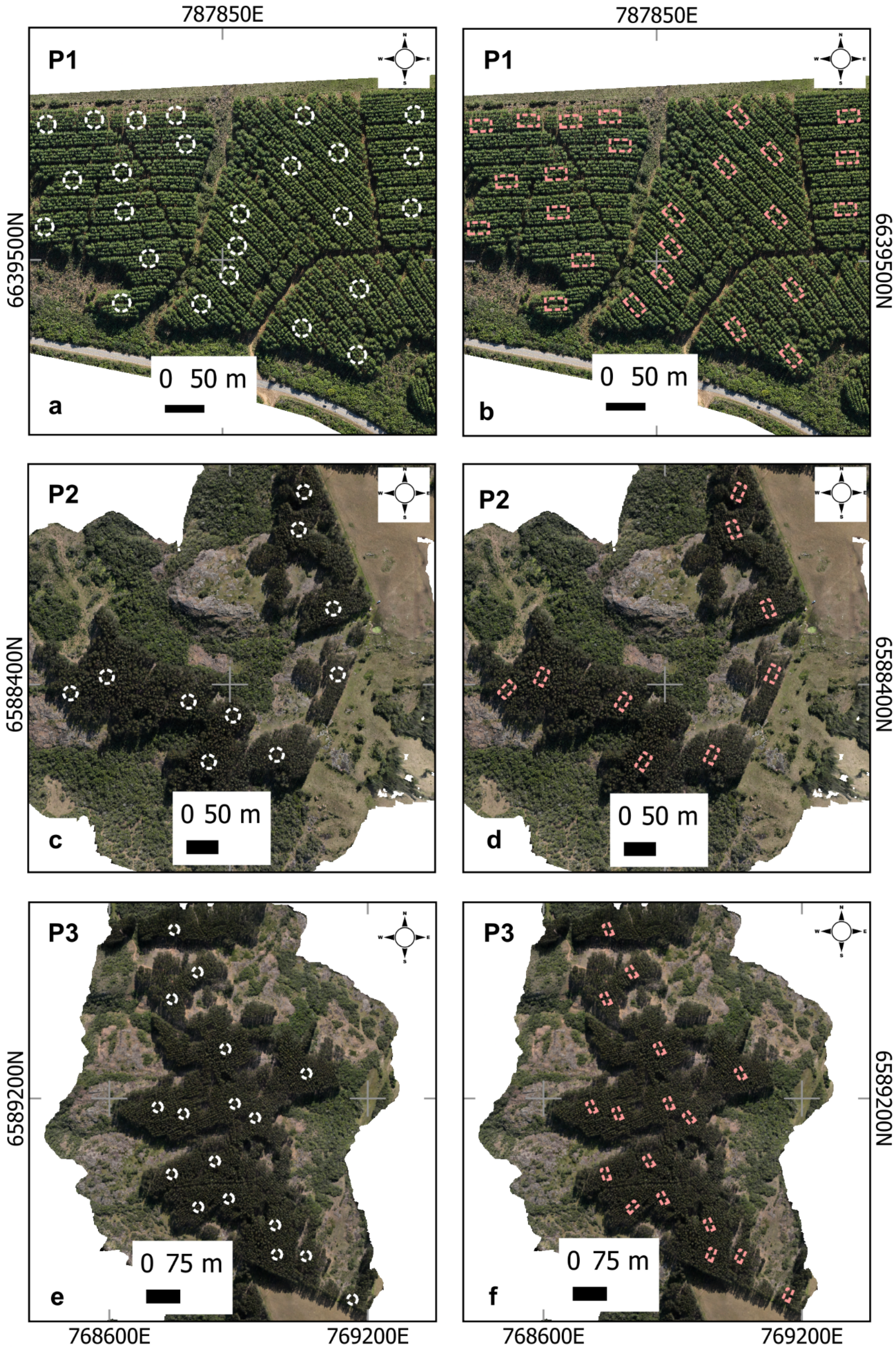

Figure 3. Location of the sample plots in the three plantations (P1, P2, and P3), overlaid on the orthomosaics generated for the *Pinus* and *Eucalyptus* plantations in the municipalities of Santa Margarida do Sul and Lavras do Sul, RS.

Legend: a: location of circular sample plots in P1; b: location of rectangular sample plots in P1; c: location of circular sample plots in P2; d: location of rectangular sample plots in P2; e: location of circular sample plots in P3; f: location of rectangular sample plots in P3. UTM Coordinate System, SIRGAS 2000 Datum, Zone 21S.

When the p-value was < 0.05, comparisons were performed using nonparametric methods. Accordingly, the nonparametric Mann–Whitney U test (Bauer, 1972; Hollander & Wolfe, 1973) was used to compare two groups. No data treatments were applied to remove outliers prior to the statistical analyses.

3. Results and Discussion

3.1 Forest inventory

In the *Pinus* area (P1), field measurements were carried out using a conventional forest inventory, totaling 854 trees distributed across 25 sampling units. For descriptive statistical analysis, 270 trees were used, for which the variables height (H) and diameter at breast height (DBH) were measured. A total of 1,055 RGB images were generated, with a ground sampling distance (GSD) of 3.75 cm/pixel.

In the *Eucalyptus* areas (P2 and P3), diameter at breast height (DBH) was measured for all individuals within the sampling units in both areas. In P2, 418 trees were recorded, totaling 0.4 hectares, while in P3, 885 trees were measured over a total area of 0.8 hectares. Regarding total height, 134 trees were measured in P2 and 261 in P3. Based on the sampling, the sampling units showed average values of 42 and 45 trees for P2 and P3, respectively, corresponding to estimated densities of 1,045 and 1,106 trees per hectare. During the survey, a total of 755 images were generated, with a ground sampling distance (GSD) of 3.97 cm·pixel^{-1}.

3.2 Exploratory analysis

The mean, median, first and third quartiles of the tree count values for area P1 (Figure 1c; Figure 3a and b) are presented in Table 3.

Table 3. Exploratory statistical analysis of the number of trees for P1, P2, and P3.

Area	Statistic	Field	Circular	Rectangular
P1	1st Quartile	29.00	20.00	22.00
	Median	31.00	26.00	25.00
	Mean	30.88	26.60	26.80
	3rd Quartile	34.00	33.00	29.00
P2	1st Quartile	33.75	26.00	28.50
	Median	43.00	28.50	32.50
	Mean	41.80	30.30	33.30
	3rd Quartile	46.75	36.50	36.75
P3	1st Quartile	36.00	25.00	23.75
	Median	41.00	26.50	26.00
	Mean	42.44	26.88	26.19
	3rd Quartile	45.75	29.25	28.00

The exploratory data analysis for P1 indicates that the circular counting method exhibits the greatest data dispersion, as evidenced by an interquartile range of 13 trees, whereas the field and rectangular methods, considering the same metric, showed lower values of 5 and 7, respectively. When the same metric is considered for P2, it is again observed that the field method presents the largest interquartile range, with a value of 13 trees, while the circular method shows 10.5 trees and the rectangular method 8.25 trees. For P3, a similar pattern was observed, with the largest interquartile range recorded for the field method (9.75 trees), compared with 4.25 trees for both the circular and rectangular methods (Table 3 and Figure 3).

The differences evidenced by this metric may suggest that it is not a good indicator for comparing the number of trees, since the largest interval was observed for the circular counting method in area P1, rather than for the field method, as observed in P1 and P2.

The behavior observed for P2 and P3, which have different planting spacings, may indicate an underestimation of the number of trees when counts are performed using images obtained by UAVs.

In part, this can be explained by the fact that, in the field, it is possible to clearly identify each individual tree, whereas in images, confusion may occur among overlapping or adjacent crowns, precisely due to the characteristics of the measured species. According to Hastings et al. (2020), the accuracy of tree crown detection depends on crown shape. Trees with more spread-out crown forms show higher overall detection accuracy, while species with different morphological characteristics tend to present lower accuracy (Hastings et al., 2020).

This confusion may be intensified when planting distances are shorter. According to Zarco-Tejada et al. (2020), one of the reasons this method has difficulty detecting individual trees is the close proximity of trees planted near each other (spacing).

Another noteworthy detail is that the medians are very close to the means across the three methods and the three plantations (P1, P2, and P3) (Table 3 and Figure 4), which reinforces the hypothesis that the means can represent, with good approximation, the population of each method studied in each plantation. The differences did not exceed 1.5 trees (min = 0.12 and max = 1.44 trees).

It is possible to observe, through the exploratory analysis considering Figure 5 (P3), that there is a greater divergence between the alternative tree-counting methods when compared to the traditional method. It is also important to highlight the possible occurrence of an outlier in area P3 for tree counting using the circular method.

When analyzing the assumption of data normality using the Shapiro–Wilk test (SHAPIRO, S. S. & WILK, M. B., 1965; ROYSTON, 1982a; ROYSTON, 1982b; ROYSTON, 1995), the following p-values were obtained: P1, p-value = 0.243; P2, p-value = 0.404; P3, p-value = 0.0007. Therefore, based on these results, it is not possible to state that the P3 sample comes from a population that follows a normal distribution. For P1 and P2, however, it can be stated that the samples come from populations with a normal distribution. Based on these assumptions, Student's *t*-test was applied to compare the three methods in

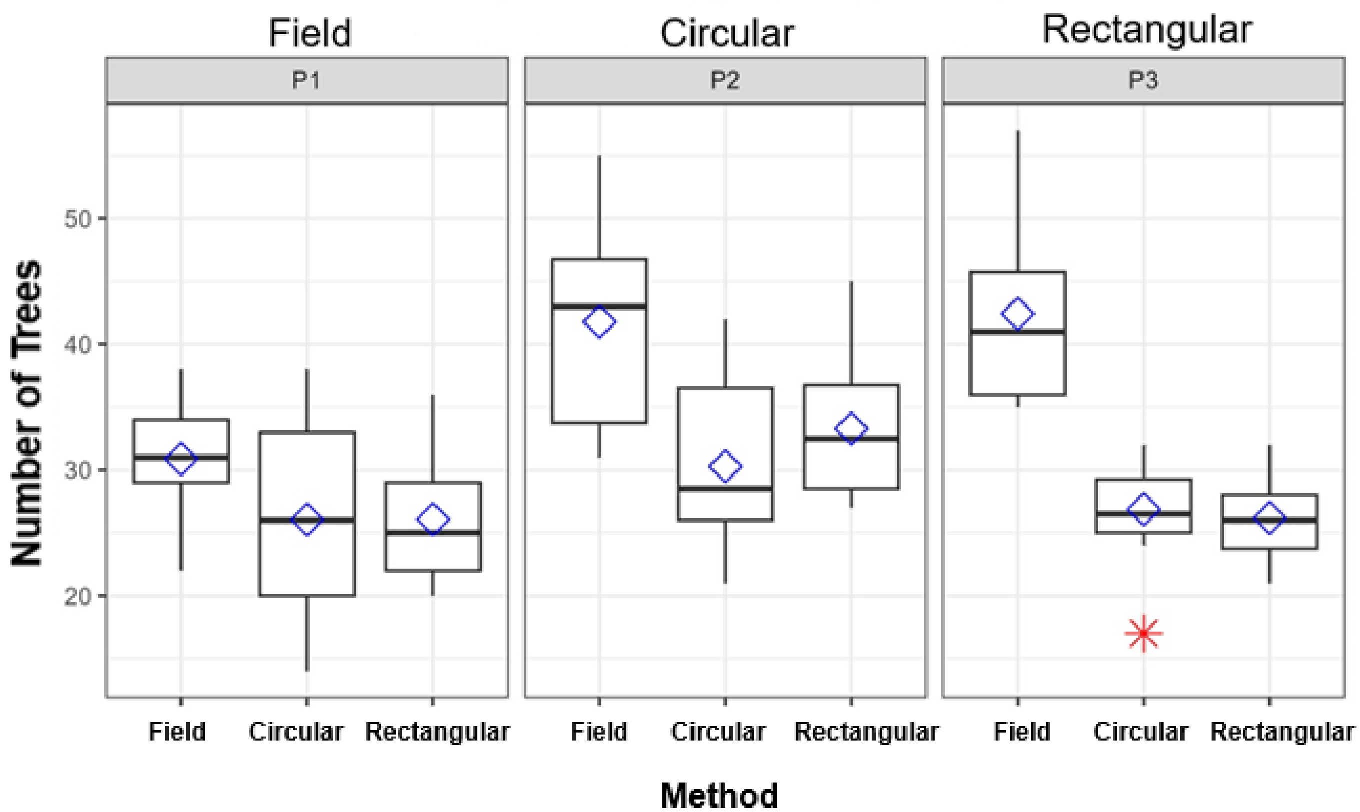

Figure 4. Boxplot showing the mean values of each method in blue for areas P1, P2, and P3.

Legend: red asterisks indicate the presence of outliers.

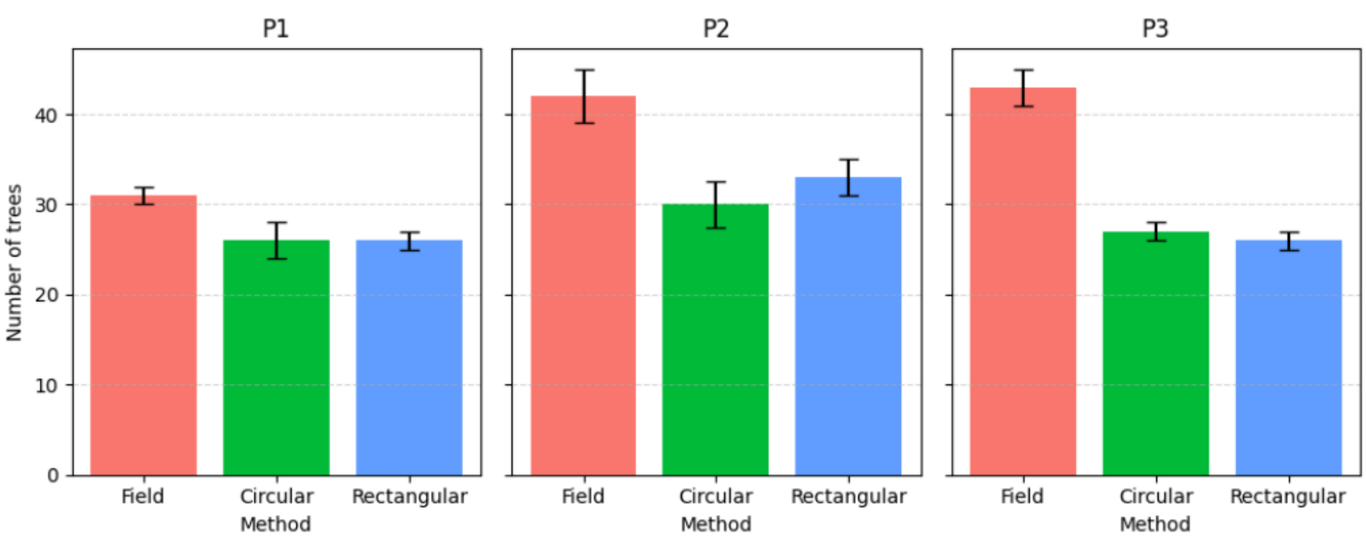

Figure 5. Bar chart showing the mean values of trees counted by each method and their error deviations for areas P1, P2, and P3.

areas P1 and P2, while for P3 the nonparametric Mann–Whitney U test was used (BAUER, 1972; HOLLANDER & WOLFE, 1973).

3.3 Comparison of methods

The comparison between the methods, using Student's *t*-test for P1 and P2, as well as the nonparametric Mann–Whitney U test, resulted in the outcomes presented in Table 4.

Table 4. *p*-values obtained from Student's *t*-tests (P1 and P2) and the Mann–Whitney U test (P3) for method comparison.

	P1			P2			P3		
	Field	Circular	Rectangular	Field	Circular	Rectangular	Field	Circular	Rectangular
Field	–	0.000	0.001	–	0.002	0.010	–	0.000	0.000
Circular	0.000	–	0.992	0.002	–	0.311	0.000	–	0.393
Rectangular	0.001	0.992	–	0.010	0.311	–	0.000	0.393	–

Legend: Field = Field method; Circular = Circular plot; Rectangular = Rectangular plot.

Based on the statistical tests applied, it was possible to observe that the field method differed from the data collection methods using UAV-acquired images, both in the circular and rectangular formats. However, the UAV-based methods did not differ statistically from each other. These results were consistent across the three study areas, P1, P2, and P3.

It is observed that, in numerical terms, when comparing the means among the three methods for the different species, the means obtained from field data showed the greatest differences when compared with the means from the alternative methods (circular and rectangular) for P2 and P3, to the detriment of the differences between the field and the circular and rectangular methods in P1. The differences between the obtained means, expressed as number of trees, are presented in Table 5.

Table 5. Differences between the obtained means, expressed as number of trees.

	P1			P2			P3		
	Field	Circular	Rectangular	Field	Circular	Rectangular	Field	Circular	Rectangular
Field	–	4.28	4.08	–	11.50	8.50	–	15.56	16.25
Circular	4.28	–	0.20	11.50	–	3.00	15.56	–	0.69
Rectangular	4.08	0.20	–	8.50	3.00	–	16.25	0.69	–

Legend: Field = Field method; Circular = Circular plot; Rectangular = Rectangular plot.

The differences observed in the means reinforce the hypothesis that tree counting for different species using alternative methods (circular and rectangular) may present smaller discrepancies in mean values for *Pinus* (P1) than for *Eucalyptus* (P2 and P3). The greater range observed for P2 and P3 can be explained by the difficulty in clearly identifying individual trees in the orthomosaic due to crown architecture, even under different planting spacings.

According to Nevalainen et al. (2017), the use of remote sensing through (UAVs) offers great potential for accurate results in the automatic identification of trees and species classification. However, its performance may be compromised when images are acquired under variable lighting and shadow conditions.

Although the statistical tests indicate significant differences among the means, for P1 the alternative UAV-based methods present similar mean values at approximately 86%. For P2 and P3, the means are similar to the field values, ranging from approximately 72% to 80% for P2 and from 61% to 63% for P3. This reinforces the hypothesis that tree-counting methods should be species-specific.

Another factor identified as influencing tree detection and count estimation was reported by Alexander et al. (2018), who observed that area topography also plays a role in tree detection in their study based on LiDAR-derived data.

4. Conclusion

It was observed that, for both *Pinus* sp. and *Eucalyptus* sp., alternative methods based on the use of UAVs are not efficient for sample-based determination of the number of trees in the plantation, regardless of whether circular or rectangular sampling formats are used.

UAV-based methods may present larger differences between mean values for different species when compared to field data. Therefore, it is recommended that counting studies using alternative methods be conducted with approaches specific to each species. It is understood that the inefficiency of the method is mainly related to image quality, which is often affected by unfavorable climatic conditions, making visual counting difficult. Thus, for the continuation of studies within this context, it is suggested that flights be carried out at lower altitudes and that image processing be performed at higher quality. Another relevant factor is planting density, since canopy overlap also hinders the distinction between individual trees.

For tree counting using alternative UAV-based methods, the sampling format (rectangular or circular) does not influence the tree count.

Acknowledgments

No acknowledgments were declared for this work.

Author Statements

✓ No conflicts of interest were declared.

✓ All existing funding sources were acknowledged.

✓ This article is released under the Creative Commons Attribution License (CC-BY).

✓ There is no evidence of plagiarism in this article.

References

Alexander, C.; Korstjens, A. H.; Hill, R. A. (2018). Influence of micro-topography and crown characteristics on tree height estimations in tropical forests based on LiDAR canopy height models. International Journal of Applied Earth Observation and Geoinformation, v. 65, p. 105–113.

AGISOFT. (2020). Agisoft Metashape. User Manual: Professional Edition, Version 1.6, September.

Dalla Corte, A. P.; Souza, D. V.; Rex, F. E.; Sanquetta, C. R.; Mohan, M.; Silva, C. A.; Zambrano, A. M. A.; Prata, G.; Almeida, D. R. A.; Trautenmüller, J. W.; Klauberg, C.; Moraes, A.; Sanquetta, M. N.; Wilkinson, B.; Broadbent, E. N. (2020). Forest inventory with high-density UAV-Lidar: Machine learning approaches for predicting individual tree attributes. Comput. Electron. Agric., v. 179, p. 10-14, 2020.

David F. B. (1972). Constructing confidence sets using rank statistics. Journal of the American Statistical Association 67, 687–690. doi:https://doi.org/10.1080/01621459.1972.10481279.

DJI. Manual de instruções Mavic 3M. 2023. Disponível em: https://dl.djicdn.com/downloads/DJI_Mavic_3_Enterprise/20230531/DJI_Mavic_3M_UM-pt-br_v1.2.pdf. Acesso em: 15 julho. 2025

Figueiredo, E. O.; Figueiredo, S. M. De M.; Neves D'oliveira, M. V.; Santos, E. K. M. (2018). Manejo florestal 4.0: calendário preliminar de inventário florestal com aeronaves remotamente pilotadas. Rio Branco, AC: Embrapa Acre, 56 p.

Han, P.; Ma, C.; Chen, J.; Chen, L.; Bu, S.; Xu, S.; Zhao, Y.; Zhang, C.; Hagino, T. (2022). Fast Tree Detection and Counting on UAVs for Sequential Aerial Images with Generating Orthophoto Mosaicing. Remote Sensing, v. 14, n. 16, p. 4113, ago. DOI: https://doi.org/10.3390/rs14164113.

Hastings; J. H.; Ollinger, S. V.; Ouimette, A. P.; Sanders-DeMott, R.; Palace, M. W.; Ducey, M. J.; Sullivan, F. B.; Basler, D.; Orwig, D. A. (2020). Tree species traits determine the success of LiDAR-based crown mapping in a mixed temperate forest. Remote Sensing, v. 12, p. 309, 2020.

Hofmann-Wellenhof, B.; Lichtenegger, H.; Collins, J. (2001). Global Positioning System: Theory and Practice. 5. ed. Vienna: Springer Vienna. DOI: https://doi.org/10.1007/9783709161999.

INSTITUTO BRASILEIRO DE GEOGRAFIA E ESTATÍSTICA (IBGE). (2012). Caracterização da vegetação do Brasil. Rio de Janeiro: IBGE. Disponível em: https://www.ibge.gov.br. Acesso em: 17 set. 2025.

Kusnandar, T. (2020). Penggunaan Unmanned Aerial Vehicle untuk Pemetaan Lahan Wisata Desa Sindang Pakuwon Parakan Muncang. INTERNAL (Information System Journal), 3(1). https://doi.org/10.32627/internal.v3i1.300

Macedo, W. (1984). Levantamento do reconhecimento dos solos do município de Bagé, RS. Disponível em: https://www.infoteca.cnptia.embrapa.br/infoteca/handle/doc/219834. Acesso em: 17 set 2025.

Monico, J. F. G. (2008). Posicionamento Pelo GNSS: Descrição, Fundamentos e Aplicações. In Editora Unesp: Vol. 2a Edição.

Moreno, J. A. (1961). Clima do Rio Grande do Sul. Porto Alegre: Secretaria da Agricultura, 35 p.

Myles H.; and Douglas A. Wolfe (1973). Nonparametric Statistical Methods. New York: John Wiley & Sons. Pages 27–33 (one-sample), 68–75 (two-sample). Or second edition (1999).

MSRS, Museu de Solos do Rio Grande do Sul. Solos do Rio Grande do Sul. (1973). Disponível em: https://www.ufsm.br/museus/msrs/unidade-de-solos. Acesso em: 17 set. 2025.

Nevalainen, O.; Honkavaara, E.; Tuominen, S.; Viljanen, N.; Hakala, T.; Yu, X.; Hyyppä, J.; Saari, H.; Pölönen, I.; Imai, N. N.; Tommaselli, A. M. G. (2017). Individual Tree Detection and Classification with UAV-Based Photogrammetric Point Clouds and Hyperspectral Imaging. Remote Sensing, v. 9, n. 3, p. 185.

Pinto, L. O. R.; Dantas, Daniel; T., M. C. N. S.; Mello, J. M.; Cabacinha, C. D. (2024). Custo, tempo e precisão: uma otimização do inventário florestal pré-corte em um povoamento de eucalipto. Pesquisa Florestal Brasileira, [S. l.], v. 44. DOI: 10.4336/2024.pfb.44e202102251. Disponível em: https://pfb.cnpf.embrapa.br/pfb/index.php/pfb/article/view/2251. Acesso em: 12 abr. 2025.

QGIS Development Team. (2021). Welcome to the QGIS project! In QGIS Geographic Information System.

Raffaelli, J. A. (2022). Geoprocessamento aplicado na análise do espaço geográfico do município de Santa Margarida do Sul - RS. Dissertação (Mestrado em Geografia) — Universidade Federal de Santa Maria, Santa Maria, 2002.

R Core Team (2025). _R: A Language and Environment for Statistical Computing_. R Foundation for Statistical Computing, Vienna, Austria. https://www.R-project.org.

Royston, P. (1982)_a. An extension of Shapiro and Wilk's W test for normality to large samples. Applied Statistics, 31, 115–124. doi:https://doi.org/10.2307/2347973.

Royston, P. (1982)_b. Algorithm AS 181: The W test for Normality. Applied Statistics, 31, 176–180. doi: https://doi.org/10.2307/2347986.

Royston, P. (1995). Remark AS R94: A remark on Algorithm AS 181: The W test for normality. Applied Statistics, 44, 547–551. doi: https://doi.org/10.2307/2986146.

Shapiro, S. S. And Wilk, M. B. (1965). An analysis of variance test for normality. Biometrika, 52, 591-611.

Sousa, H. L. (2017). Sensoriamento Remoto com VANTs: uma nova possibilidade para a aquisição de geoinformações. Revista Brasileira de Geomática, v. 5, n. 3, p. 326-342.

Zarco-Tejada, P. J.; Ruiz-Verdu, A.; Ruiz-Verdu, M.; Ruiz-Verdu, J. (2020). Detecting and counting orchard trees on unmanned aerial vehicle (UAV)-based images using entropy and NDVI features. ISPRS Archives, v. XLIII-B2, p. 1211–1218. DOI: https://doi.org/10.5194/isprs-archives-XLIII-B2-2020-1211-2020.